



Enormous impulsive enhancement of particle fluxes observed on Aragats on May 23, 2023

A. Chilingarian*, G. Hovsepyan, B. Sargsyan, T. Karapetyan, D. Aslanyan, L. Kozliner

Alikhanyan National Lab (Yerevan Physics Institute), Yerevan 0036, Armenia

Received 3 October 2023; received in revised form 18 February 2024; accepted 21 February 2024

Abstract

An unprecedented thunderstorm ground enhancement (TGE) event was recorded on May 23, 2023, at Aragats Mountain, the highest peak in Armenia. This event showcased a maximum flux intensity surpassing 3 million particles per minute per square meter for energies above 0.4 MeV. Distinctly, the fluence of the event was measured at approximately ≈ 700 particles/cm². The comprehensive instrumentation at the Aragats research station, including a suite of spectrometers and detectors, enabled precise cross-correlation of measurements. The electron flux at energies exceeding 10 MeV was observed at roughly $\approx 55,000$ particles per minute per square meter. Additional measurements, including cloud base heights and corona discharge detections, validated the intensity of the electric field, reaching approximately 2.1 kV/cm at elevations 50–100 m above ground level. Our observations confirm that TGE is a universal and significant atmospheric event, contributing a substantial flux of high-energy electrons to the global electrical circuit. Integrating such TGE phenomena into Earth's numerical models is imperative, considering their impact on aviation and aerospace operation safety. © 2024 COSPAR. Published by Elsevier B.V. All rights reserved.

Keywords: eosinophilic esophagitis; HEPA; TGE; RREA; NGR; Atmospheric Electric field; Spectrometer

1. Introduction

The developing domain of High Energy Physics in Atmosphere (HEPA, [Dwyer et al., 2012](#)) delves into how cosmic ray flux modulation by electric fields affects the Earth's atmosphere, encompassing phenomena such as thunderstorm ground enhancements (TGEs, [Chilingarian et al., 2010,2011](#)), terrestrial gamma-ray flashes (TGFs, [Fishman et al., 1994](#)), and gamma-ray glows ([McCarthy and Parks, 1985](#); [Tsuchiya et al., 2007](#), [Kelley et al., 2015](#)). Central to atmospheric high-energy phenomena is the acceleration of electrons within atmospheric electric fields. Electrons from extensive air showers (EASs, [Auger et al., 1939](#)) can attain net energy gains in the presence of sufficiently strong electric fields, giving rise to particle

avalanches. This mechanism, originally termed Runaway Breakdown (RB, [Gurevich et al., 1992](#)) and now more commonly known as the Relativistic Runaway Electron Avalanche (RREA, [Babich et al., 2001](#); [Alexeenko et al., 2002](#); [Dwyer, 2007](#)), perpetuates as long as the electric field can sustain the ongoing electron-gamma ray amplification. The RREA mechanism is instrumental in multiplying particles detectable on the Earth's surface as TGEs, in space as TGFs, or the atmosphere as gamma-ray glows. The RREA is a threshold process influenced by electric field strength and air density, as elucidated by ([Dwyer, 2003](#)). On a finer scale, the modification of the electron energy spectra (MOS), as described by ([Dorman and Dorman, 2005](#)) and ([Chilingarian et al., 2012](#)), operates independently of a specific electric field threshold and is instrumental in altering particle energy spectra.

If the RREA is ended at a height of above 100 m from the ground, you may notice gamma rays only. This

* Corresponding author.

E-mail address: chili@aragats.am (A. Chilingarian).

happens because the dense air weakens the electron flux and allows only gamma rays to reach the ground in amounts, allowing the spectrum recovery. Wintertime gamma-ray glows (similar to TGEs but do not involve registering electrons) are commonly seen on the northwest coast of Japan. This occurs when cold and dry winds blow in from Siberia and mix with the Tsushima warm current, creating an upward current of air that triggers thunderstorms (Torii et al., 2011). Airborne detectors have also been picked up on these gamma-ray glows, caused by electrons being accelerated in the space between the positive layer on top of the cloud and the negative screening layer above it (Østgaard et al., 2019).

Understanding HEPA phenomena requires worldwide registration of elementary particles in the energy range of 0.3–100 MeV, accompanied by monitoring of environmental parameters by weather stations, electric field sensors, and all-sky cameras. Correlation analysis of the acquired multivariate information will help to create models of how electrons, positrons, muons, neutrons, and photons interact with the atmosphere. Physicists from the Yerevan Physics Institute, with colleagues from the SEVAN network, conducted the first-ever TGE searching campaign utilizing SEVAN detectors at the highest peaks in Eastern Europe and Germany (Chilingarian et al., 2021a). The campaign continued 24/7 for ten years and resulted in the detection of numerous TGEs at the mountains of Aragats, Lomnicky Stit, Musala, and now also at Zugspitze (Chilingarian et al., 2024). After joint analysis of these observations, it was discovered that despite a large variety of detected TGEs, their intensity, duration, and shapes, they share many common characteristics. The largest TGEs last a few minutes. During this time, particle fluxes can increase to tens or even hundreds of times the fair-weather values. TGEs are often terminated abruptly by lightning flashes (Chilingarian et al., 2015); however, during TGEs, lightning activity is suppressed (Chilingarian et al., 2017). Recently published catalogs document 650 TGE events observed on Aragats (Chilingarian et al., 2022a) and 80 gamma-ray glows detected on the western seashore of Japan (Wada et al., 2021), providing evidence that RREA is a universal mechanism operating in thunderous atmospheres across the globe.

However, there is currently a limited understanding of how electrons are accelerated in the atmosphere due to the chaotic nature of thunderstorms and the limited measurements of the quickly changing atmospheric electric field. Also, it's necessary to distinguish the measured TGE flux from other flux sources, such as CR secondary flux (background) and Radon isotopes gamma radiation. The low energy portion of the TGE spectrum can be attributed mainly to the ^{222}Rn decay chain, specifically the daughter isotopes ^{214}Bi and ^{214}Pb , which prevail in the background radiation spectrum at low energies (Chilingarian et al., 2019). ^{222}Rn isotopes, after attaching to charged aerosols, are lifted from the ground, where they emanate from basalts to the atmosphere during thunder-

storms (Radon circulation effect, Chilingarian et al., 2020). This led to additional gamma radiation contributing to the low energy part of the TGE energy spectrum. Lead filters are screening spectrometers from the Radon progeny gamma radiation, see Fig. 1.

For isotope spectroscopy, we utilize precise ORTEC's gamma spectrometer (Chilingarian et al., 2022b). Our primary goal is to recover the giant TGE's intensities, fluences, and maximum energies. Additionally, we seek to investigate the strength of atmospheric electric fields that trigger electron-photon avalanches in the atmosphere. To explore these relationships, we thoroughly examined the largest TGE ever observed on Aragats.

2. Method

We perform measurements of the changing particle fluxes and environmental parameters on the slopes of Mt. Aragats at heights 3200, 2000, and 1600 m above sea level. Various particle detectors and spectrometers monitor particle fluxes of almost all species of the secondary CR flux. We use the ORTEC-905-4 spectrometer for Natural gamma-ray radiation (NGR) spectroscopy, Fig. 1a. This gamma spectrometer is equipped with a 3" x 3" NaI (TI) crystal (cross-section of 0.0056 m²), has 1024 measuring channels, excellent stability, efficiency in registering gamma rays in the energy range 0.3 – 3 MeV \approx 50 %, and a relative energy resolution of FWHM (full width at half maximum) approximately 8 % at energy levels of 0.3–3 MeV (Hossain et al., 2012). Also, we utilize a network of six large NaI spectrometers to observe TGE gamma radiation, see in Fig. 1b two of them. The sensitive area of each spectrometer is roughly 0.035 m² (11.5 x 30 cm) with a thickness of 11.5 cm, which is about six times larger than the ORTEC spectrometer. NaI spectrometers provide ample statistics (40,000 to 50,000 counts per minute) to recover the TGE energy spectrum in the energy range of 0.3 – 50 MeV. However, the energy resolution of large NaI spectrometers at low energies is much worse than ORTEC's, and we cannot resolve the isotope spectral lines with it. Combining ORTEC with large NaI spectrometers allows us to perform accurate isotope spectroscopy within the energy range of 0.3–3 MeV and retrieve energy spectra of up to 50 MeV. For more details on the spectrometer and energy recovery method, please refer to (Chilingarian et al., 2022c).

The intensity of the TGE gamma rays and electrons and their energy spectra above 10 MeV are measured with arrays of stacked plastic scintillators 0.25 to 4 m² area and 1,3,5, 20, and 60 cm thickness. STAND1 particle detector network, located across the Aragats station, at an area of \approx 50,000 m². Three identical units of the STAND1 network are located near three main experimental halls – MAKET, SKL, and GAMMA. 1 m² area, 1 cm thick scintillators are stacked vertically, and one 3 cm thick plastic scintillator stands apart. The light from the scintillator through optical spectrum-shifter fibers is passed to the photomultiplier (PMT) FEU-115 M. The maximum

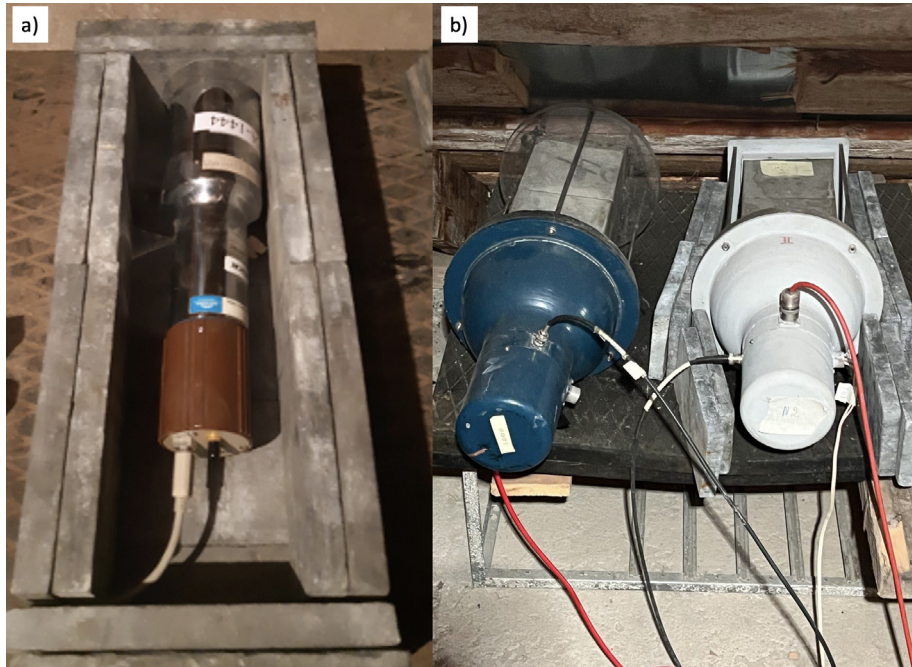


Fig. 1. A) ortec spectrometer with lead filters from the sides and the bottom; b) large nai spectrometers, one with lead filters from the sides and the bottom.

luminescence is emitted at the 420-nm wavelength, with a luminescence time of about 2.3 ns. The STAND1 detector is tuned by changing the high voltage applied to the PMT and setting the thresholds for the discriminator shaper. The discrimination level is chosen to guarantee high signal detection efficiency and maximal suppression of photomultiplier noise. The efficiency of scintillators reaches 95 % for electron energies above 10 MeV and 2 % for gamma rays with energies above 3 MeV (for the upper scintillators). The energy threshold of the upper scintillators is ≈ 1 MeV. Dead time is $\sim 0.7 \mu\text{s}$. A 50 ms time series of STAND1 detectors, synchronized with NSEF measurements and meteorological parameters, are transferred to the Cosmic ray Division (CRD) database and are available online in graphical and numerical format via the Advanced Data Extraction Infrastructure (ADEI) platform (Chilingaryan et al. (2008)).

The “STAND3” detector comprises four layers of 3-cm-thick, 1-m² sensitive area scintillators stacked vertically, using the same PMT and electronics as STAND1 detectors. In addition, DAQ electronics register and store coincidences of the signals and 1-minute histograms of energy releases for further offline analysis and online alerts issuing. If we denote by “1” the signal from a scintillator and by “0” the absence of a signal, then the following combinations of the 4-layered detector output are stored: “1000”—most probable electron energy 10 – 20 MeV; “1100”—most probable electron energy 20–30 MeV; “1110”—most probable electron energy 30–40 MeV; “1111”—above 40 MeV.

On Aragats, we install several weather stations, lightning locators, magnetometers, and electric field sensors. The Davis Vantage Pro2 weather station (DAVIS, 2024)

has multiple instruments to measure weather conditions, including a rain collector, temperature sensor, humidity sensor, anemometer, solar radiation sensor, and UV radiation sensor. A network of six field mills (Boltek EFM-100, 2024) monitors near-surface electrostatic field changes and distances to nearby lightning flashes (within 33 km). Among these field mills, three are located in Aragats station, one in Nor Amberd station (12.8 km away), another in Burakan (15 km away), and the last one in Yerevan (39 km away).

3. The largest ever TGE observed on Aragats on 23 May 2023

Particle flux enhancement on Aragats usually counts 10–20 %, rarely larger than 100 %. Most of the 369 TGEs registered in 2013–2023, and all large ones occurred in Spring and Autumn (81 %) when the outside temperature is mostly in the $-2\text{C}^\circ - +2\text{C}^\circ$ range and clouds are very low above the Aragats research station (yellow and green colors on the histogram of Fig. 2).

Approximately 12 % of TGE events occurred in Summer (rose color, mostly under black color) and 7 % in Winter (black color).

The histogram showed 369 TGE events from 11 years of observations since the electric field sensors and weather stations were installed on Aragats. In 2008–2012, 277 TGE events were observed; however, meteorological and electricity sensors were not installed. Thus, the total number of TGE events reaches ≈ 650 . The TGEs were selected if three independent particle detectors demonstrate simultaneous peaks in the count rate time series larger than 3σ and the NSEF absolute value exceeds 3 kV/m. All TGE

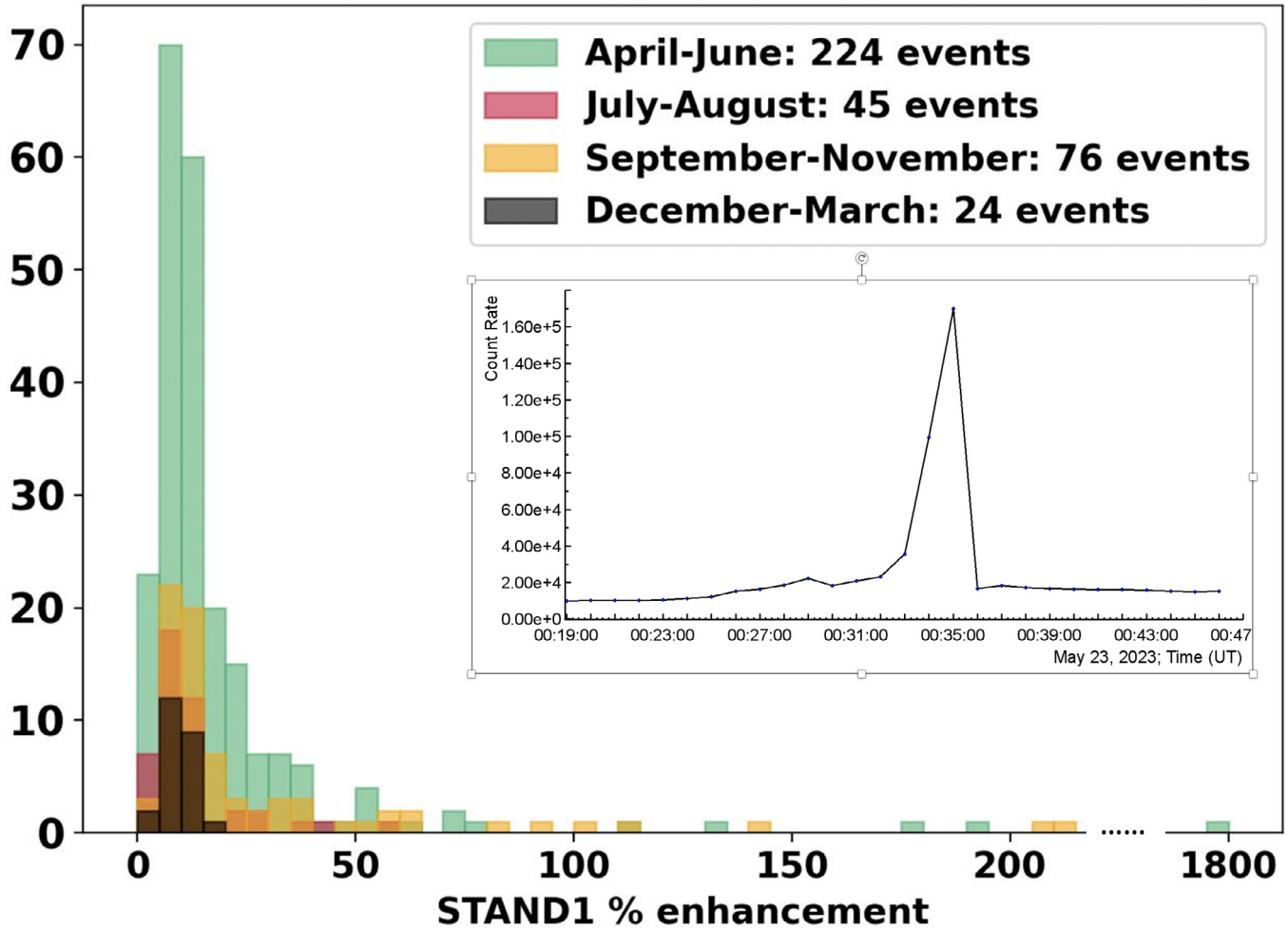


Fig. 2. The season-dependent histogram of the 369 TGE enhancements in percent. The 1 cm thick and 1 m² area plastic scintillator was used for the relative enhancement calculation. The inset shows the 1-minute time series of the scintillator count rate measured on May 23, 2023 (maximum flux was at 00:34 – 00:35).

candidates were carefully examined to exclude possible artifacts. On the right side of Fig. 2, we show the enhancement counting $\approx 1800\%$ of an extraordinarily large TGE that occurred on 23 May 2023 (corresponding count rate time series are shown in the inset). While such outliers are expected in an exceedingly large number of measurements, it is unlikely to obtain such a huge TGE in only 369 trials. Furthermore, two events well over 1000% at Lomnický štít (Chum et al., 2020) and one at Musala Mountains by the SEVAN detectors (Chilingarian et al., 2021d) are worth mentioning.

Fig. 3 shows the 1-second time series of the STAND1 network scintillator's count rate (blue curve) and NSEF (black curve) at maximum flux minute. Red lines indicate the distance to lightning flashes. During TGE, lightning activity was suppressed until, at 00:34:58, a lightning flash (at a 3 km distance) abruptly terminated it. The 50 ms count rate of the upper STAND1 detector reduced from 187 to 25, 7.5 times in 150 ms from 00:34:57.950 to 00:34:58.100. However, the TGE count rate before lightning was very stable at maximum minute flux; the relative

error was 2.8%, and at fair weather, the relative error is larger – 4.4%. Thus, an electron accelerator in the thundercloud provides a sustainable flux of relativistic electrons for a minute despite the chaotic characteristics of thundercloud charging. At the same minute, NSEF, which reflects the strength and direction of the atmospheric field electric aloft, changed from -5.2 kV/m to $+4.9$ kV/m, with a mean value of -2.4 ± 2.9 kV/m. The strength of NSEF during the stable particle flux is rather modest; 2 min earlier, NSEF was -18 kV/m. Based on the results of this remarkable TGE, it can be inferred that there is no linear relationship between NSEF and particle flux and, hence, between NSEF and the atmospheric electric field. Nevertheless, the study has revealed a certain degree of order in the atmospheric electric field that supports a stable flux lasting for a minute, which was not previously noticed.

The rain rate during TGE was 2 mm/hour, relative humidity was 98%, temperature was 0.3°C, and atmospheric pressure was 694 mbar.

In Fig. 4, we show the time series of count rates of NaI N2 and ORTEC spectrometers. Both spectrometers cannot

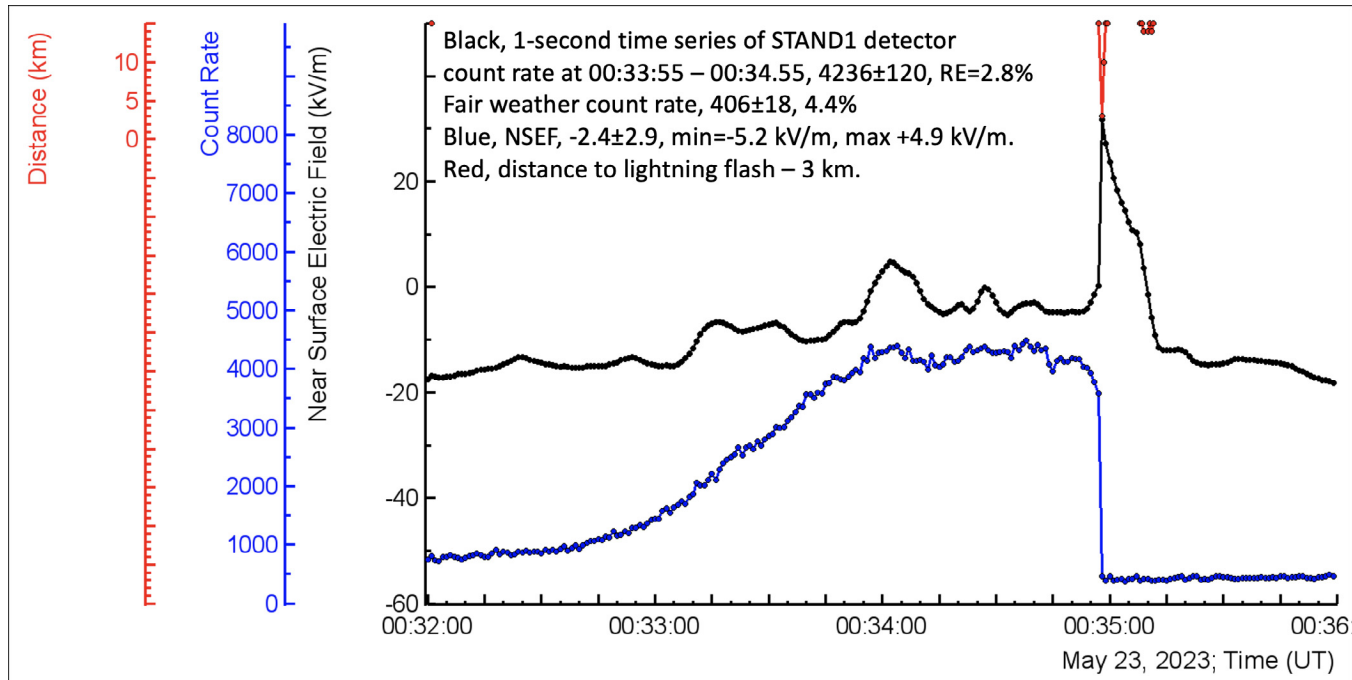


Fig. 3. TGE development in the thunderous atmosphere. Relation of particle flux to NSEF.

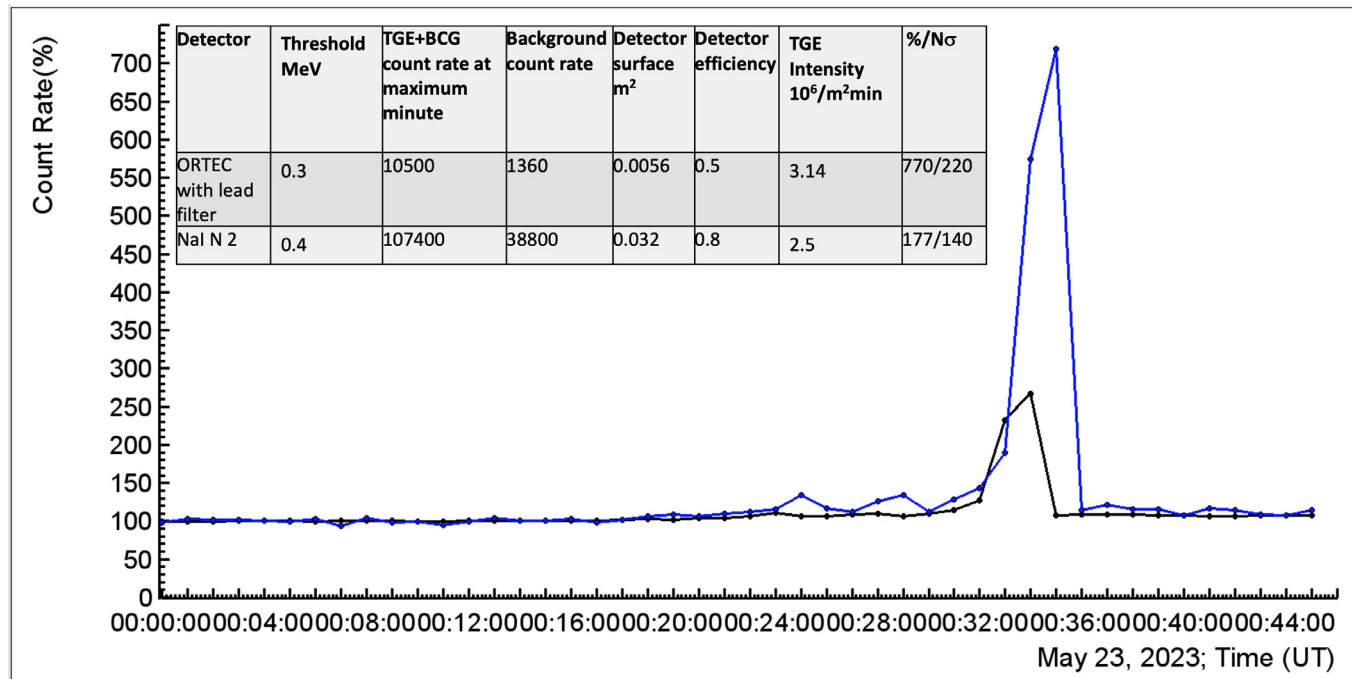


Fig. 4. 1-minute time series of count rates: NaI 2 (black) and ORTEC (blue) spectrometers. In the inset – the measurements at maximum flux minute and characteristics of spectrometers.

separate charged and neutral fluxes. Time series are shown in percent enhancement relative to values measured at fine weather before TGE. In the inset, we show the TGE intensity and spectrometer’s parameters. The last column shows the increase in flux and peak significance, measured in standard deviations relative to the background. Both spectrometers have a low energy threshold and register natural gamma radiation from basalts around the station. The

most significant contributors to gamma radiation in the radon decay chain are ²¹⁴Bi (609 keV) and ²¹⁴Pb (352 keV) isotopes. Most Aragats detectors have energy thresholds well above this energy, and NGR contamination is negligible. To suppress NGR contamination, 4 cm thick lead filters were installed around the ORTEC spectrometer on all sides and at the bottom, effectively reducing NGR. This resulted, for instance, in a ~50-fold decrease in

the intensity of the ^{214}Bi isotope. The spectrometer was open at the top, allowing TGE particles from near-vertical directions to be registered.

Fig. 5 presents the TGE integral energy spectrum during the peak flux minute, as the NaI spectrometer recorded (blue curve). The background spectrum obtained in fair weather conditions is shown in red. The numerical values of both spectra are detailed in the inset. At low energies, the TGE's intensity is 2.6 times that of the background. A notable peak in the TGE flux appears at 2–3 MeV, quadrupling the background levels, coinciding with the disappearance of radon progeny gamma radiation and a consequent decline in the background spectrum. Beyond 40 MeV, the TGE flux shows a gradual attenuation. The overall intensity of the TGE in the energy range above 0.3 MeV, as measured by both ORTEC and NaI spectrometers, is approximately 3.2 million particles per minute per square meter or 5.3 particles per second per square centimeter. The NaI detector's fluence measurement for the TGE, from 0:12 to 0:36 UT, amounts to roughly 700 particles/cm².

4. Electron flux registration by ASNT and STAND3 detectors

The TGE electron spectrum registration is vital in demonstrating the RREA development above detectors (Chilingarian et al., 2023). The Aragats Solar Neutron Telescope (ASNT) of 4 m² area measures the energy released in 5 and 60 cm thick plastic scintillator. The name of the spectrometer is historical; the detector was primarily designed to register direct neutrons originating in the corona from violent solar flares 20 years ago. The spectrometer consists of four modules, each of two stacked

scintillators of 5 cm (veto layer) and 60 cm (spectrometric layer) in thickness. Both layers have an electron registration efficiency of approximately 95 % and gamma-ray registration efficiency of 6–7 % and 40–60 %, respectively. Every 20 s, energy release histograms in both layers and energy releases corresponding to the "01" coincidence (with a veto on charged particles) are stored. The electron energy spectrum is obtained by subtracting the histogram corresponding to the "01" selection from the overall energy release histogram. We recover gamma-ray and electron energy spectra using a detailed simulation of the detector response made with the GEANT4 code (see details in Chilingarian et al., 2022d; Chilingarian et al., 2023).

First, we examine energy-release histograms in the 5 cm thick scintillator of ASNT and the 3 cm thick scintillator of STAND3 detectors to identify the presence of electrons in the TGE flux. In Fig. 6, we demonstrate the energy release histograms of all particles traversing the 3 cm thick (2a) and 5 cm thick (2b) scintillators at minute 00:34 – 00:35 on 23 May 2023. From the overall energy release histogram (green curves), we subtract histograms corresponding to the gamma-ray contribution (black curves). These histograms were obtained using the gamma-ray energy spectrum recovered by the ASNT spectrometer. Gamma rays modeled according to this spectrum were tracked through the roofs of the buildings and detectors till registration. For the ASNT response simulation, we used a 50 % enlarged gamma-ray spectrum to compensate for gamma rays absorbed by wet snow on the roof of the MAKET experimental hall. The residual red curves represent the distribution of energy releases of the TGE electrons in the 3 and 5-cm thick scintillators. The electron losses in the scintillator are ≈ 1.8 MeV per centimeter; consequently, the energy release in a 3-cm thick scintillator peaked at

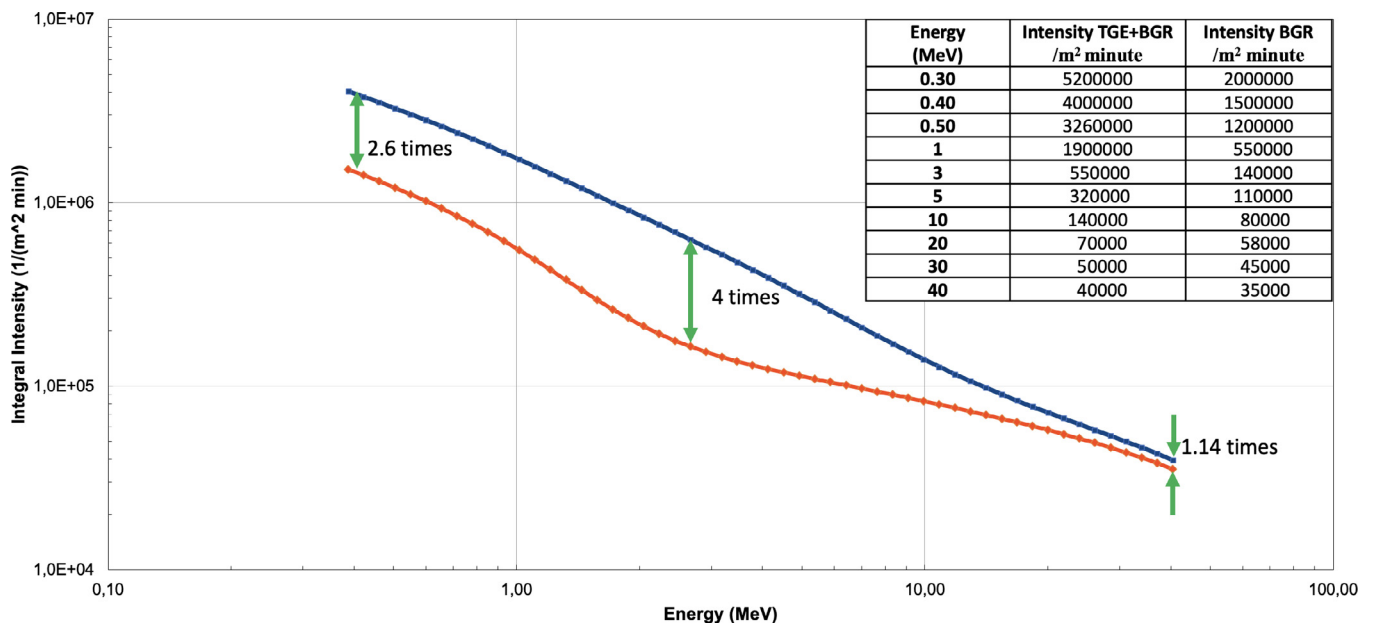


Fig. 5. The TGE integral energy spectrum (blue line) recovered from the NaI N2 spectrometer and background spectrum (red line). In the inset, we show numerical values of TGE flux intensity.

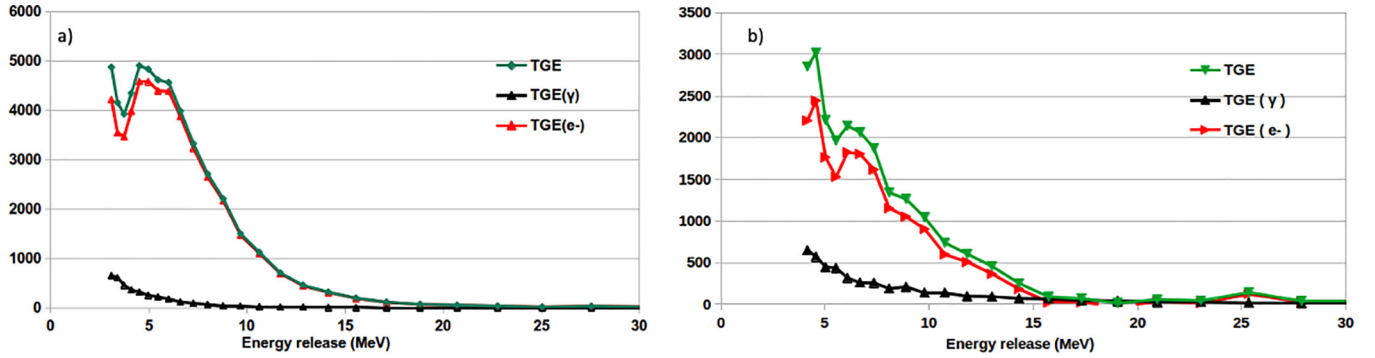


Fig. 6. Energy release histograms in 3-cm thick a) and 5-cm thick b) scintillators. Green – all particles; black – simulated gamma-ray contribution; red – electron flux energy releases.

4–6 MeV, and in 5-cm thick – at 6–8 MeV. Large peaks in the distributions indicate a significant number of electrons in the TGE.

The analysis of count rates and energy release histograms typically offers insights into the high-energy electron energy flux. Under normal circumstances, the ASNT spectrometer is used to determine the spectrum, which is then corroborated by STAND3 data. However, on May 23, a significant discrepancy arose between these two detectors’ readings. This inconsistency was attributed to the wet snow covering the roof of the MAKET experimental hall, which affected the detectors’ response. Thus, the energy spectra from the ASNT spectrometer are not presented because due to TGE electron flux absorption and scattering, compromising the spectrum’s reliability.

In contrast, the SKL experimental hall, situated 100 m from the MAKET hall, remained clear of snow and thus unaffected by such biases. Thus, we present an electron energy spectrum from STAND3 measurements. Fig. 7 illustrates the rough estimate of the electron energy spectrum obtained by STAND3 “1000,” “1100,” and “1110” coincidence configurations, each indicative of different minimum energy thresholds. The “1111” coincidence, associated with the highest energy, was excluded due to potential contamination from the modification of the MOS process (Chilingarian et al., 2012). The gamma-ray detection efficiency of 3 cm thick scintillators is too low for accurate energy spectrum analysis. The energy spectrum obtained by 3 points is insufficient for confirming electron flux. Luckily, a CUBE scintillation spectrometer with sizes (0.5 x 0.5 x 0.2 m³) operates in the SKL hall next to STAND3. This spectrometer has a veto option for separating charged and neutral fluxes; more details about the CUBE detector are provided (Chilingarian et al., 2024). In the next section, we will present the energy spectrum obtained by the CUBE spectrometer.

5. Location of atmospheric electric field within thundercloud

The standard cloud electrification due to warm air updraft and following suspended hydrometeor interactions

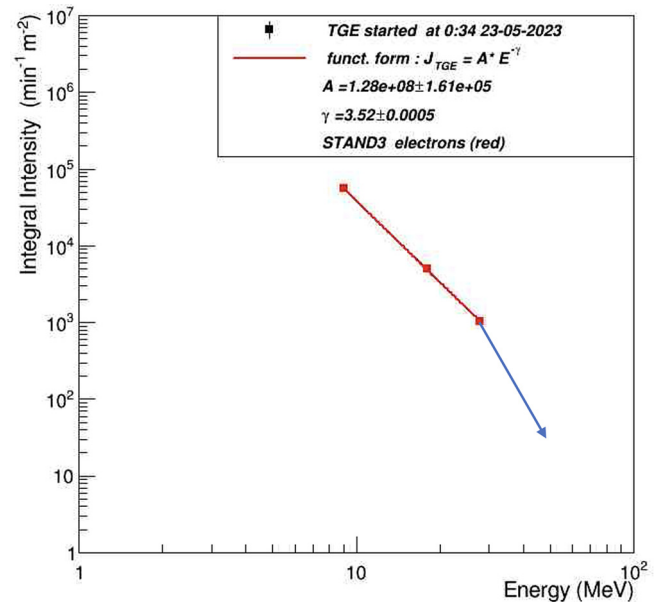


Fig. 7. Electron energy spectrum recovered by STAND3 detector’s coincidences. The blue arrow pointed to the electrons registered by the “1111” coincidence.

led to the charge separation and emergence of the lower dipole accelerated electrons downward. We accept the tri-pole model of the electrostatic field of a thunderstorm according to Kuettner measurements at the Zugspitze in 1945–1949 (Kuettner, 1950). The threshold electric field for the RREA was estimated to be $(2.83\text{--}3.05) \times n$ kV/cm, where n is the air density relative to that at sea level (Roussel-Dupré et al., 1998). Dwyer (2003) further investigated the avalanche threshold (critical field strength) and found it to be:

$$E_{th} = 2.84 \times n \text{ kV/cm} \quad (1)$$

in agreement with Babich’s value of $2.83 \times n$ kV/cm (Babich et al., 2004). This threshold field is slightly higher than the breakeven field, the minimum ionization energy loss. If the electrons traveled exactly along the electric field lines, this would be the threshold for runaway electron propagation and avalanche multiplication. Nevertheless,

the electrons' trajectories deviate due to Coulomb scattering with atomic nuclei and Møller scattering with atomic electrons, causing deviations. Additionally, secondary electrons from Møller scattering aren't created along the field line, so 10–20 % larger electric fields are necessary for electrons to run away and make an avalanche. Thus, if we apply Eq. (1) to RREA above Aragats station, we will obtain the required intracloud electric field of 1.8 – 1.9 kV/cm on 5–6 km heights and 2.0 – 2.1 kV/cm at ≈ 3000 km heights, see Fig. 2 of (Chilingarian et al., 2021b). The potential strengths and locations of the intracloud electric field were confirmed during multiple simulations of the RREA development above particle detectors (Chilingarian et al., 2021c). Obtained in simulations, fluxes of electrons and gamma rays were compared with TGE count rates (Chilingarian et al., 2022e). Observing several electron energy spectra on Aragats, we reveal at least 2.1 kV/cm intracloud electric fields at 50–100 m altitudes above the Earth's surface (Chilingarian and Hovsepian, 2022f).

To reliably detect “super electron events,” as termed by Williams et al. (2023), the presence of an accelerating electric field extending below 100 m above ground level is essential, as detailed by Chilingarian et al. (2023). For localizing the atmospheric electric field above spectrometers, we introduce an approximate equation based on measured maximum energies of electrons and gamma rays as they reach the detection level. An empirical Eq. (2) determines the distance the strong accelerating field terminates and the RREA avalanche leaves the intracloud electric field (free path distance, FPD, Chilingarian, et al., 2021b). The equation parameters were fitted by simulations.

$$\text{FPD (meters)} = (C1 * E_{\text{max}}^e - E_{\text{max}}^c) / C2 \quad (2)$$

Coefficients C1 and C2 are estimated to be 1.2 and 0.2, respectively. TGE simulations suggest that the maximum energy of electrons going out of the electric field is ≈ 20 % higher than that of gamma rays. Therefore, we can estimate the maximum energy of electrons leaving the field by $C1 * E_{\gamma}^{\text{max}}$. Furthermore, we assume that the maximum energy of gamma rays does not change significantly when they travel 100 m or less in the atmosphere above detectors. Also, we assume that electrons lose approximately 0.2 MeV per m at altitudes of about 3000 m. We conducted multiple simulations of electron-gamma ray avalanches to verify the accuracy of Eq. (2) and detect any potential methodological errors. We store the particle energies and solve the inverse problem to recover the RREA characteristics from the TGE parameters. To achieve this, we utilize CORSIKA simulations with varying electric field strengths and termination heights. Subsequently, we apply all experimental procedures to the obtained samples to estimate the maximum energies of electrons and gamma rays. Once we have calculated the FPD parameter, we compare it to the “true” value in the simulation. Based on this comparison, we estimate the method's standard error to be 50 m. In Fig. 8, we pre-

sent the integral energy spectra of electrons and gamma rays recovered by the energy release histograms measured by the CUBE detector at the maximum TGE flux (Chilingarian et al., 2024). The maximum energies of electrons and gamma rays are 45 and 49 MeV, respectively. From Eq. (2), we derive the mean free path distance to be ≈ 70 m.

The cloud base height is estimated by calculating the difference between the air temperature and dew point provided by Davis weather station according to the well-known approximate Eq. (3) (Cloud base, 2024). The difference (spread) between the air temperature and the dew point indicates how much cooling is needed for condensation. This method assumes a linear and uniform decrease in temperature with altitude, which might not always be the case in real atmospheric conditions with local variations.

$$H(\text{m}) \approx (\text{Air temperature at surface } \{^{\circ}\text{C}\} - \text{dew point temperature } \{^{\circ}\text{C}\}) \times 122 \quad (3)$$

Fig. 9a maps the relationship between cloud base height and outside temperature, drawing on data from 369 TGE events recorded at Aragats in 2013–2023. During Spring and Autumn—when the most intense TGEs occur, as highlighted in green and yellow—the temperature bracket of -2°C to $+2^{\circ}\text{C}$ covers the vast majority of electron-dominant TGEs. Corresponding cloud base heights are frequently below 100 m, often dipping under 50 m. This pattern is exemplified by the TGE event on May 23, depicted in Fig. 9b, where the external temperature was -0.2°C and the cloud base height was estimated to be around 35 m.

The FPD ≈ 70 m and cloud base ≈ 35 m point to the presence of an atmospheric electric field below 100 m, which is pivotal for facilitating the descent of RREA to the ground, thereby significantly contributing to the TGE with an appreciable electron content. The deduced electric field gradient is extraordinarily steep, transitioning from -210 kV/m at 50–100 m above the surface to mere kV/m a few meters above the ground. The pronounced nature

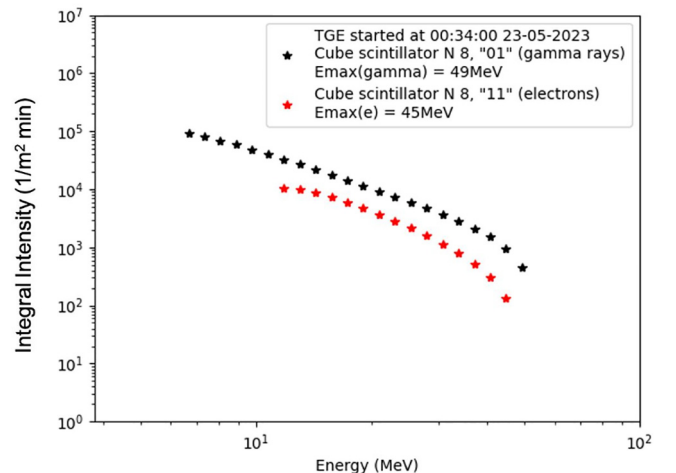


Fig. 8. Integral energy spectra of electrons (red) and gamma-rays (black) at maximum minute flux recovered from the CUBE spectrometer.

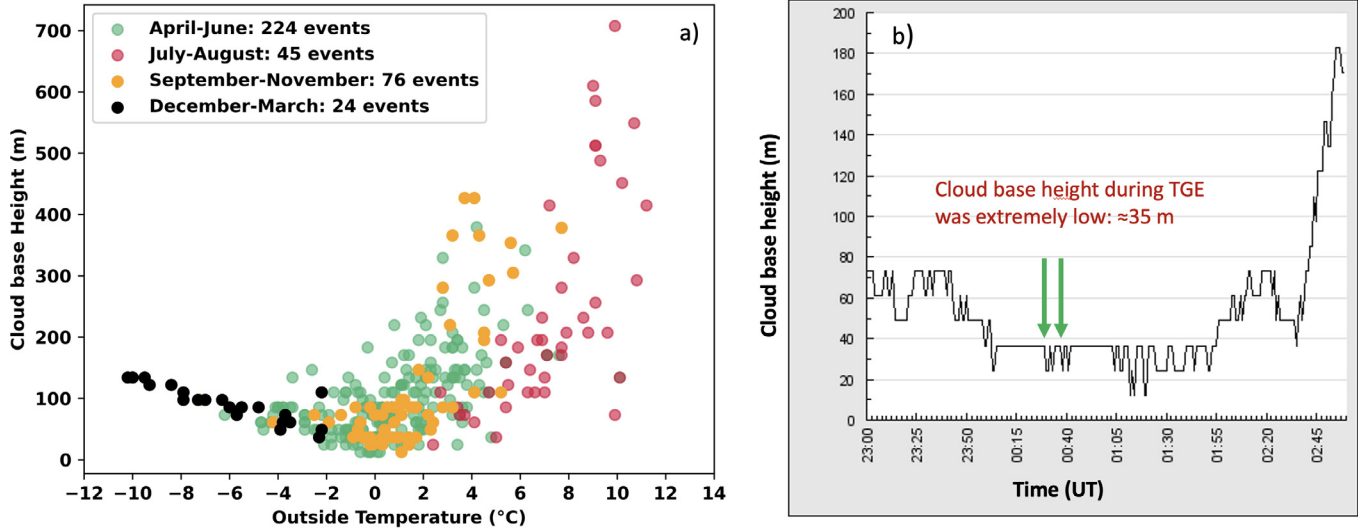


Fig. 9. a) the scatter plot of cloud base estimates vs. the outside temperature. the data is available from the tge events catalog of the last decade (369 tge available from mendeley dataset [29]); b) time series of cloud base height estimated from outside temperature and dew point measured by the davis weather station on may 23, 2023.

of this gradient intimates a highly concentrated charge distribution within the cloud, capable of engendering a marked potential difference across a relatively short vertical distance. A nearby (3 km away) lightning flash notably diminished the potential difference, abruptly ending the TGE. Such sharp electric field gradients are typically observed near the Earth’s surface, marking areas where conductivity shifts from the air to the ground.

Fig. 10 highlights an additional observation: rare light glows, typically observed 2–3 times per year, as captured by panoramic cameras overseeing the skies above Aragats

station (Chilingarian et al., 2022g). For sky surveillance, we deploy ALL SKY CAM model cameras from Moonglow Technologies (AllSkycam, 2024), featuring a 190-degree hemispherical field of view via a circular fisheye system. The hardware comprises a Color 1/3" Sony Super HAD CCD II image sensor with an automatic exposure range from 10⁻⁵ to 4 s and a resolution of 546 × 457 pixels across the field of view.

Corona discharges, which can occur when the atmospheric electric field intensifies, are typically seen near sharp metallic structures. At standard conditions of

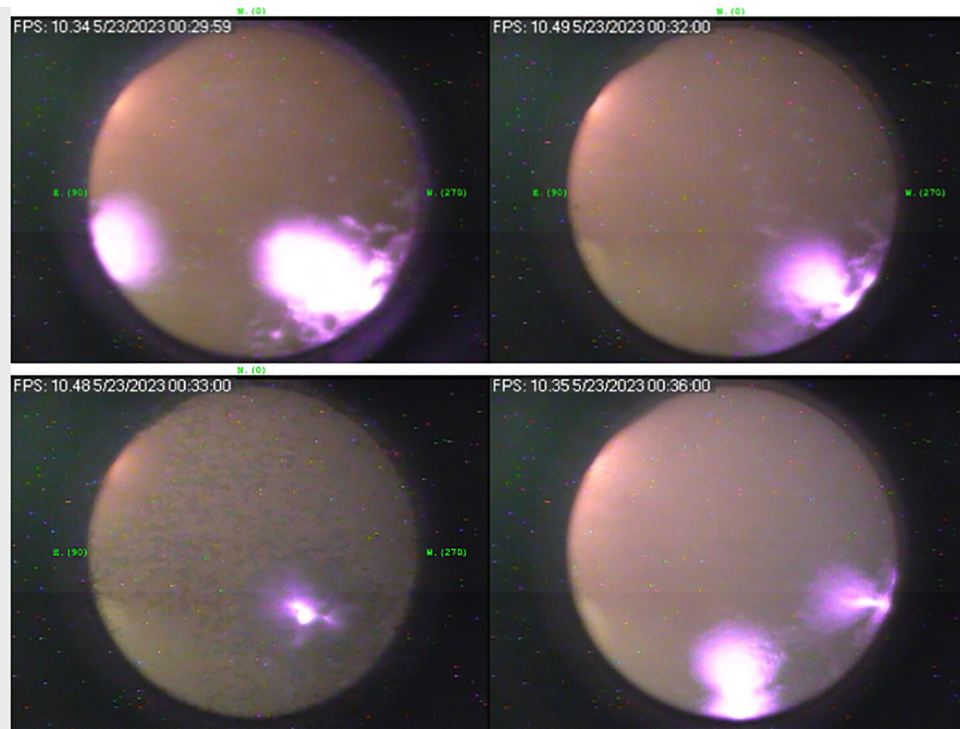


Fig. 10. The light glows occurred during the maximum minutes of TGE (00:30–00:36).

1 atm and 20 °C, the electric field threshold for corona inception in a uniform field is around 20–30 kV/cm. This threshold can be lower near sharp edges and at higher altitudes where the decreased air pressure reduces the necessary electric field strength for a corona discharge to occur. As Earle Williams recently suggested (Williams et al., 2023), fast positive ions from corona discharges could contribute to an increased potential drop in the lower dipole. The corona discharges captured by the camera at the edges of the field of view at 00:30, 00:32, and 00:36 could be attributed to discharges from metallic masts near the station. However, the air glows detected near the center of the field of view cannot be ascribed to corona discharges, and their exact nature remains a topic of scientific inquiry. Notably, the light glow recorded at 00:33 coincides with the peak in atmospheric electron flux, suggesting that these electrons' interaction with atmospheric molecules may trigger this unique transient luminous event.

6. Conclusions

On May 23, 2023, the Aragats station recorded an unprecedented TGE event—the most substantial in 15 years of observations. The particle flux enhancement, measured by a 1 cm thick plastic scintillator, dramatically increased, registering 1800 % above baseline. NaI and ORTEC spectrometers detected an overwhelming flux of over 3 million particles per minute per square meter. Notably, the electron flux intensity for energies above 10 MeV reached approximately 55,000 particles per minute per square meter.

The strength of the electric field reached 2.1 kV/cm at heights \approx 50 m above the ground. Specific atmospheric conditions delayed lightning initiation for minutes, permitting the RREA process to persist longer than usual, which resulted in the substantial TGE observed. This finding suggests that, in addition to the lightning low-energy electron current, there are also significant, minute-stable, relativistic electron currents related to thunderstorms distributed across the globe.

These phenomena have profound implications for the global electric circuit (GEC), affecting the Earth's electrical environment. Additionally, large near-surface electric fields can trigger corona discharges, threatening rocket launches and charging processes. Therefore, numerical models of Earth's atmospheric processes must incorporate TGE events as a standard occurrence during thunderstorms to improve the accuracy and reliability of predictions and safety protocols.

Declaration of Competing Interest

The authors declare that they have no known competing financial interests or personal relationships that could have appeared to influence the work reported in this paper.

Acknowledgments

The data for this paper are available via the multivariate visualization software ADEI on the Cosmic Ray Division (CRD) web page of the Yerevan Physics Institute (ADEI, 2024). We thank Gurgen Gabaryan, Karen Asatryan, and Edik Arshakyan for maintaining the ASNT, Na(Tl), ORTEC spectrometers, and Suren Chilingarian for developing the ADEI data analysis platform. The authors acknowledge the support of the Science Committee of the Republic of Armenia (Research Project No. 21AG-1C012) in the modernization of the technical infrastructure of high-altitude stations.

References

- ADEI, available online: <http://adei.crd.yerphi.am/> (accessed on 1 January 2024).
- Alexeenko, V.V., Khaerdinov, N.S., Lidvansky, A.S., et al., 2002. Transient variations of secondary cosmic rays due to atmospheric electric field and evidence for pre-lightning particle acceleration. *Phys. Lett. A* 301, 299–306.
- AllSkycam, available online: <http://www.moonglowtech.com/products/AllSkyCam/Weather.shtml> (accessed on 1 January 2024).
- Auger, P., Ehrenfest, P., Maze, R., et al., 1939. Extensive cosmic-ray showers. *Rev. Mod. Phys.* 11 (3–4), 288–291.
- Babich, L.P., Donskoy, E.N., Kutsyk, I.M., et al., 2001. *IEEE Trans. Plasma Sci.* 29 (3), 430–438.
- Babich, L.P., Donskoy, E.N., Il'kaev, R.I., Kutsyk, I.M., Roussel-Dupre', R.A., 2004. *Plasma Phys. Rep.* 30, 616–624.
- BOLTEK, available online: https://www.boltek.com/EFM-100C_Manual_030323.pdf (accessed on 1 January 2024).
- Chilingarian, A., Hovsepyan, G., & Sargsyan, B. (2020). Circulation of Radon progeny in the terrestrial atmosphere during thunderstorms. *Geophysical Research Letters*, 47, e2020GL091155. <https://doi.org/10.1029/2020GL091155>.
- Chilingarian A., Hovsepyan G., Karapetyan T., et al. (2022d) Multi-messenger observations of thunderstorm-related bursts of cosmic rays, 2022 *JINST* 17 P07022.
- Chilingarian, A., Hovsepyan G., Karapetyan T., Sargsyan B., Svechnikova, E. (2022g) Transient Luminous Events in the Lower Part of the Atmosphere Originated in the Peripheral Regions of a Thunderstorm Universe, 8, 412. <https://doi.org/10.3390/universe8080412>.
- Chilingarian, A., Hovsepyan, G., Aslanyan, D., Karapetyan, T., Sargsyan, B., & Zazyan, M. (2023). TGE electron energy spectra: Comment on “radar diagnosis of the thundercloud electron accelerator” by E. Williams et al. (2023) *Journal of Geophysical Research: Atmospheres*, 128, e2022JD037309. <https://doi.org/10.1029/2022JD037309>.
- Chilingarian, A., Hovsepyan, G., Zazyan, M., 2021b. Measurement of TGE particle energy spectra: An insight in the cloud charge structure. *Europhys. Lett.* 134, 6901. <https://doi.org/10.1209/0295-5075/ac0dfa>.
- Chilingarian, A., Hovsepyan, G., Svechnikova, E., Zazyan, M., 2021c. Electrical structure of the thundercloud and operation of the electron accelerator inside it. *Astropart. Phys.* 132, 102615.
- Chilingarian, A., Hovsepyan, G., Karapetyan, G., Zazyan, M., 2021d. Stopping muon effect and estimation of the intracloud electric field. *Astropart. Phys.* 124, 102505.
- Chilingarian, A., Hovsepyan, G., Karapetyan, T., Kozliner, L., Chilingarian, S., Pokhsranyan, D., Sargsyan, B., 2022b. The horizontal profile of the atmospheric electric fields as measured during thunderstorms by the network of NaI spectrometers located on the slopes of Mt. Aragats, *JINST* 17, P10011.
- Chilingarian, A., Hovsepyan, G., Karapetyan, T., Sargsyan, B., Chilingarian, S., 2022c. Measurements of energy spectra of relativistic

- electrons and gamma-rays avalanches developed in the thunderous atmosphere with Aragats solar neutron telescope. *J. Instrum.* 17, P03002.
- Chilingarian, A., Hovsepyan, G., Karapetyan, T., et al., 2022e. (2022e) Development of the relativistic runaway avalanches in the lower atmosphere above mountain altitudes. *EPL* 139, 50001. <https://doi.org/10.1209/0295-5075/ac8763>.
- Chilingarian, A., Hovsepyan, G., 2022f. Dataset for 16 parameters of ten thunderstorm ground enhancements (TGEs) allowing recovery of electron energy spectra and estimation the structure of the electric field above earth's surface. *Mendeley Data V1*. <https://doi.org/10.17632/tvbn6wdf85.2>.
- Chilingarian, A., Daryan, A., Arakelyan, K., et al., 2010. Ground-based observations of Thunderstorm-correlated fluxes of high-energy electrons, gamma rays, and neutrons. *Phys. Rev. D* 82, 043009.
- Chilingarian, A., Hovsepyan, G., Hovhannisyanyan, A., 2011. Particle bursts from thunderclouds: Natural particle accelerators above our heads. *Phys. Rev. D* 83, 062001.
- Chilingarian, A., Mailyan, B., Vanyan, L., 2012. Recovering the energy spectra of electrons and gamma rays coming from the thunderclouds. *Atmos. Res.* 114–115, 1.
- Chilingarian, A., Hovsepyan, G., Khanikyanc, Y., Reymers, A., Soghomonyan, S., 2015. Lightning origination and thunderstorm ground enhancements terminated by the lightning flash. *EPL* 110, 49001.
- Chilingarian, A., Khanikyants, Y., Mareev, E., Pokhsranyan, D., Rakov, V.A., Soghomonyan, S., 2017. Types of lightning discharges that abruptly terminate enhanced fluxes of energetic radiation and particles observed at ground level. *J. Geophys. Res. Atmos.* 122, 7582–7599.
- Chilingarian, A., Hovsepyan, G., Elbekian, A., Karapetyan, T., Kozliner, L., Martoian, H., Sargsyan, B., 2019. Origin of enhanced gamma radiation in thunderclouds. *Phys. Rev. Research* 1, 033167.
- Chilingarian, A., Karapetyan, T., Zazyan, M., Hovsepyan, G., Sargsyan, B., Nikolova, N., Angelov, H., Chum, J., Langer, R., 2021a. Maximum strength of the atmospheric electric field. *Phys. Rev. D* 103, 043021.
- Chilingarian, A., Kozliner, L., Sargsyan, B., Soghomonyan, S., Chilingaryan, S., Pokhsranyan, D., Zazyan, M., 2022a. Thunderstorm ground enhancements: multivariate analysis of 12 years of observations. *Phys. Rev. D* 106, 082004.
- Chilingarian, A., Karapetyan, T., Sargsyan, B., Knapp, J., Walter, M., Rehm, T., 2024. Energy spectra of the first TGE observed on Zugspitze by the SEVAN light detector compared with the energetic TGE observed on Aragats. *Astropart. Phys.* 156, 02924–02934. <https://doi.org/10.1016/j.astropartphys.2024.102924>.
- Chilingaryan, S., Chilingarian, A., Danielyan, V., Eppler, W., 2008. The Aragats data acquisition system for highly distributed particle detecting networks. *J. Phys. Conf. Ser.* 119, 082001.
- Chum, R., Langer, J., Baše, M., Kollárik, I., Strhářský, G., Diendorfer, J. R., 2020. Significant enhancements of secondary cosmic rays and electric field at high mountain peak during thunderstorms. *Earth Planets Space* 72, 28.
- CLOUD BASE, available online: <https://www.omnicalculator.com/physics/cloud-base> (accessed on 1 January 2024).
- DAVIS weather station, available online: <https://www.davisweatherstation.com/> (accessed on 1 January 2024).
- Dorman, L.I., Dorman, I.V., 2005. Possible influence of cosmic rays on climate through thunderstorm clouds. *Adv. Space Res.* 35, 476–483.
- Dwyer, J.R., 2003. A fundamental limit on electric fields in air. *Geophys. Res. Lett.* 30, 2055.
- Dwyer, J.R., 2007. Relativistic breakdown in planetary atmospheres. *Phys. Plasmas* 14, 042901.
- Dwyer, J.R., Smith, D.M., Cummer, S.A., 2012. High-energy atmospheric physics: terrestrial gamma-ray flashes and related phenomena. *Space Sci. Rev.* 173, 133–196.
- Fishman, G.J., Bhat, P.N., Mallozzi, R., et al., 1994. Discovery of intense gamma-ray flashes of atmospheric origin. *Science* 264, 1313–1316.
- Gurevich, A.V., Milikh, G.M., Roussel-Dupre, R.A., 1992. Runaway electron mechanism of air breakdown and preconditioning during a thunderstorm. *Phys. Lett.* 165A, 463.
- Hossain, I., Sharip, N., Viswanathan, K.K., 2012. Efficiency and resolution of HPGe and NaI(Tl) detectors using gamma-ray spectroscopy. *Sci. Res. Essays* 7 (1), 86.
- Kelley, N.A., Smith, D.M., Dwyer, J.R., et al., 2015. Relativistic electron avalanches as a thunderstorm discharge competing with lightning. *Nat. Commun.* 6 (7845).
- Kuettner, J., 1950. The electrical and meteorological conditions inside thunderclouds. *J. Meteorol.* 7, 322–332.
- McCarthy, M., Parks, G., 1985. Further observations of X-rays inside thunderstorms. *Geophys. Res. Lett.* 12, 393–396.
- Østgaard, N., Christian, H.J., Grove, J.E., Sarria, D., Mezentsev, A., Kochkin, P., et al., 2019. Gamma-ray glow observations at 20 km altitude. *J. Geophys. Res. Atmos.* 124, 7236–7254. <https://doi.org/10.1029/2019JD030312>.
- Roussel-Dupré, R., Symbalisty, E., Taranenko, Y., Yukhimuk, V., 1998. *J. Atmos. Sol.-Terr. Phys.* 60, 917–940.
- Torii, T., Sugita, T., Kamogawa, M., et al., 2011. Migrating source of energetic radiation generated by thunderstorm activity. *Geophys. Res. Lett.* 38, L24801.
- Tsuchiya, H., Enoto, T., Yamada, S., et al., 2007. Detection of high-energy gamma rays from winter thunderclouds. *Phys. Rev. Lett.* 99, 165002–165007. <https://doi.org/10.1103/PhysRevLett.99.165002>.
- Wada, Y., Matsumoto, T., Enoto, T., et al., 2021. Catalog of gamma-ray glow during four winter seasons in Japan. *Phys. Rev. Res.* 3, 043117–043151. <https://doi.org/10.1103/PhysRevResearch.3.043117>.
- Williams, E., Mailyan, B., Karapetyan, G., & Mkrtychyan, H. (2023) Conditions for energetic electrons and gamma rays in thunderstorm ground enhancements, *JGR Atmosphere*, 128, e2023JD039612. <https://doi.org/10.1029/2023JD039612>.